

## CesrTA LOW EMITTANCE TUNING\*

D. Rubin, D. Sagan, J.P. Shanks, Y. Yanay, Cornell University, Ithaca, NY 14850, USA

### Abstract

Low emittance tuning and characterization of electron cloud phenomena are central to the CesrTA R&D program. A small vertical emittance is required in order to be sensitive to the emittance-diluting effects of the electron cloud. We have developed techniques to systematically and efficiently compensate optical and alignment errors that are the sources of vertical emittance. Beam-based measurements are utilized for centering Beam Position Monitors (BPMs) with respect to adjacent quadrupoles, determining relative gains of BPM button electrodes, and measuring BPM tilts. These calibrations allow for precision measurement of transverse coupling and vertical dispersion. Achieving low emittance also requires the tune plane be relatively clear of nonlinear coupling resonances associated with sextupoles. We report on tests of a sextupole distribution designed to minimize resonance-driving terms. We also report on beam-based measurements of sextupole strengths.

### BEAM BASED QUADRUPOLE CENTER MEASUREMENT

The Beam Position Monitors (BPMs) are referenced with respect to the center of their adjacent quadrupole magnets. Magnet survey and repositioning is an ongoing process, therefore it is essential that beam-based calibration of BPM offsets require a minimum of beam time. The new CesrTA BPM system[1] allows for simultaneous measurement of the orbit and betatron phase at each BPM. With this measurement technique, orbit and phase data taken at two quadrupole settings can be combined quickly to accurately determine the quadrupole center with respect to BPM center. This reduces the number of orbit difference measurements that need to be taken, and therefore reduces the time required to center BPMs.

The procedure for centering quadrupoles is illustrated in Figure 1-3.

1. Begin with a model of the lattice. Measure the orbit and betatron phase and fit the model betatron phase advance to the measured phase advance by varying the strengths of the model quadrupoles as shown in Fig. 1. This will be referred to as the base fit.
2. Change the strength of the target quadrupole in the machine and remeasure phase and orbit. In the model, vary the strength of that quadrupole until the newly-measured and model phases agree as shown in Fig. 2.

3. Horizontal and vertical kicks are superimposed on the target quadrupole. Starting from the model fit to the second data set, vary these kicks such that the modeled orbit difference matches the measured difference as shown in Fig. 3.

The orbit difference  $dx$  is

$$dx(s) = (\tilde{x} - x_0(\bar{s}))dK_1L \frac{\sqrt{\beta(s)\beta(\bar{s})}}{2 \sin \pi\nu} \cos(|\phi(s) - \phi(\bar{s})| - \pi\nu)$$

and the quadrupole center is given by

$$\tilde{x} = \frac{\text{kick}}{L dK_1} + x_0(\bar{s})$$

The ability to simultaneously measure the orbit and betatron phase provides a fast and accurate method for measuring quadrupole centers with respect to BPMs. This technique avoids problems with hysteresis and quadrupole calibration inaccuracies. Presently, a single iteration of this procedure takes roughly 20 seconds.

### BEAM-BASED MEASUREMENT OF BPM ELECTRODE GAINS AND TILTS

Non-uniformity in the response of BPM electrodes and physical misalignment or tilts of the BPMs will introduce a systematic error into measurements of coupling and vertical dispersion. We can determine the relative gain of the four electrode BPMs by sampling the response of the electrodes to a beam that is scanned over the cross-section of the BPM[2]. The sampling is accomplished by resonantly exciting the horizontal and vertical normal modes of the beam and collecting turn-by-turn position measurements. The best-fit gains based on three distinct sets of turn-by-turn data are combined and shown in Figure 4.

The distribution of the fitted gains is shown in Figure 5

#### Determination of BPM tilts

The transverse coupling is measured by resonant excitation of the horizontal and vertical normal modes. Measurement of the relative phase and amplitude of the motion at the normal mode frequencies at each of the BPMs gives the  $\bar{C}_{11}$ ,  $\bar{C}_{12}$ , and  $\bar{C}_{22}$  elements of the coupling matrix. The measured coupling after correcting  $\bar{C}_{12}$  but before gain correction is shown in Figure 6. Coupling after gain correction is shown in Figure 7.  $\bar{C}_{12}$  measures the out-of-phase component of the coupling and is therefore very nearly independent of BPM tilts.  $\bar{C}_{11}$  and  $\bar{C}_{22}$  measure the in-phase components. If  $\bar{C}_{12}$  is small, then  $\bar{C}_{22}$  is a measure of the BPM tilt. We may therefore fit the gain-corrected coupling data to determine BPM tilts. The fitted tilts are shown in Figure 8.

\* Work supported by the National Science Foundation and by the US Department of Energy under contract numbers PHY-0734867 and DE-FC02-08ER41538.

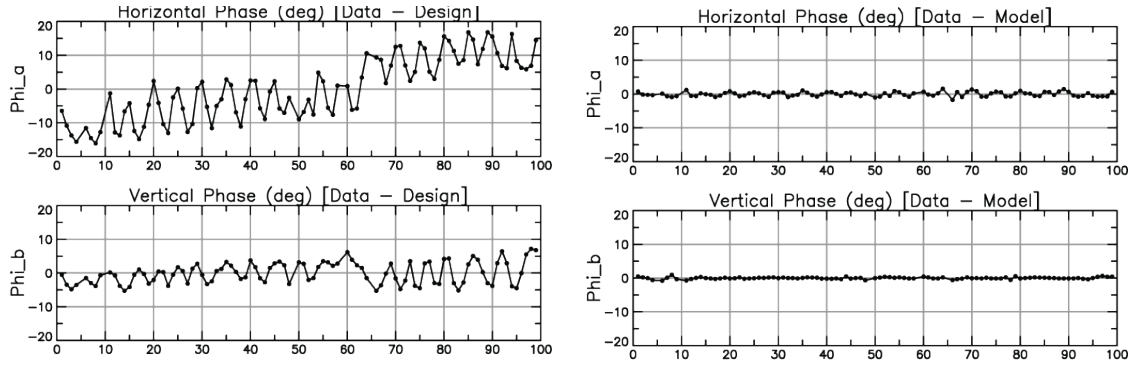


Figure 1: Vary the strengths of all quadrupoles in the lattice model until the model betatron phase matches the measured phase for the nominal  $K_1$  of the quadrupole being calibrated. This is referred to as the “base fit”. Left: Difference between the measured horizontal and vertical betatron phase and the design values of the phase. Right: Difference between the measured and the fitted model values.

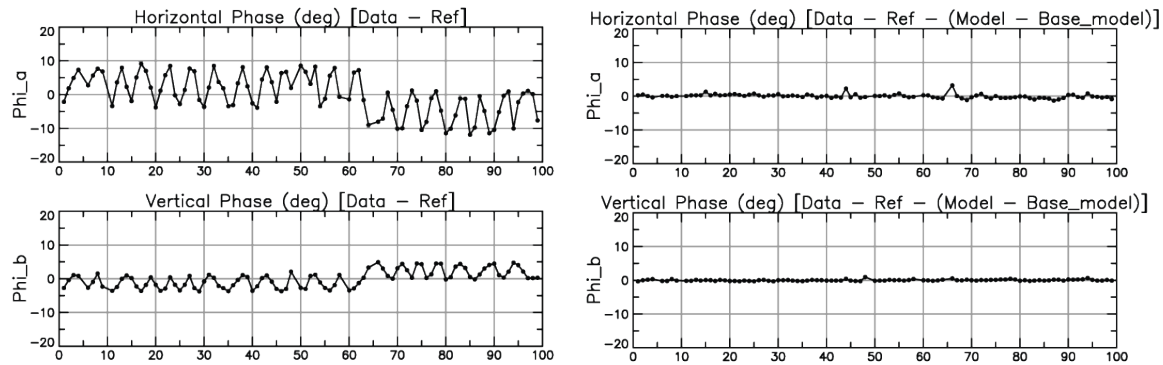


Figure 2: The strength of the target quadrupole is varied in the machine, and the phase and orbit are remeasured. The  $K_1$  of the target quadrupole is varied in the model until the modeled phase most nearly matches the measured phase. Left: Difference in phase between the measurements. Right: Difference between measured and fitted differences.

### Measurement of Vertical Dispersion

The effect of gain errors and BPM tilts on the measurement of vertical dispersion are subtle but discernible. We measure vertical dispersion by longitudinally exciting the beam at the synchrotron tune and measuring phase and amplitude of the resulting horizontal and vertical motion at each of the beam position monitors. Figure 9 shows an example of a vertical dispersion measurement without correction of BPM gain errors or BPM tilts. Transverse coupling and vertical dispersion have been jointly minimized through an optimization of skew quadrupoles and vertical steerings. The standard deviation of the residual is 20mm. (Recall that vertical dispersion is nominally zero) The same data is shown in Figure 10, now including correction of BPM button gains. The residual is reduced to 18mm. Finally, we include the fitted BPM tilts (from Figure 11), and the residual is further reduced to 17mm.

### SEXTUPOLE RESONANCES AND TURN-BY-TURN DATA

To first order, the transverse motion of a freely oscillating beam is characterized by the tunes,  $Q_x$  and  $Q_y$ , and the linear Twiss parameters. Nonlinear components such as sextupole magnets introduce higher-order resonances at frequencies  $Q_{nonlin} = nQ_x + mQ_y$ . We can extract a phase and amplitude of the beam’s response at the frequencies  $Q_{nonlin}$  from turn-by-turn data collected at all BPMs. An example of the Fourier spectrum from the horizontal position at one BPM is shown in Figure 12. The logarithmic plot of the Fourier spectrum of 4096 turns clearly shows the dominant response at  $Q_x$ , as well as the nonlinear response at higher harmonics.

The nonlinear effects of the sextupoles can be modeled using normal form analysis. The in-phase component of the horizontal response at  $2Q_x$  is shown in Figure 13. The blue line denotes the measurement at each beam position monitor and the red line shows the model analytic calculation.

Figure 14 shows the difference in the in-phase compo-

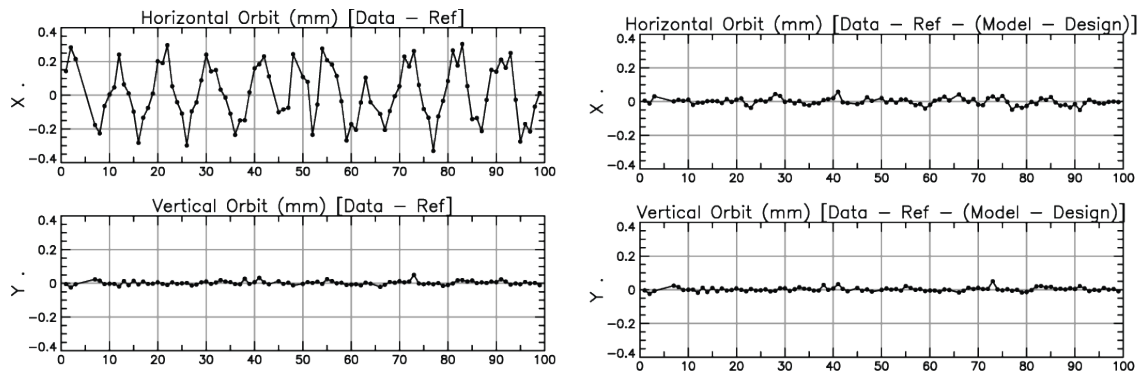


Figure 3: SHorizontal and vertical kicks are superimposed on the target quadrupole. Starting from the model fit to the second data set, vary these kicks such that the modeled orbit difference matches the measured difference. Left: Difference in measured orbits due to the change in the quadrupole strength. Right: Difference between measurement and best-fit orbit generated by the vertical kickers.

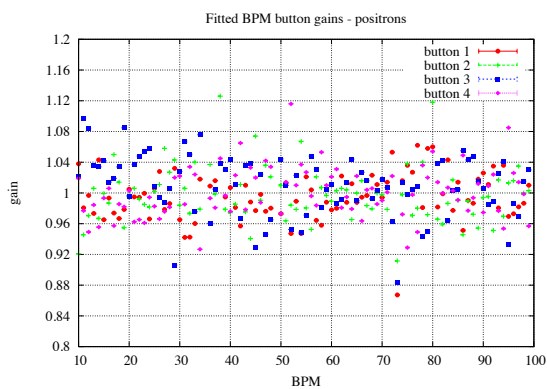


Figure 4: Fitted BPM electrode gains based on turn-by-turn data for a positron beam. The horizontal and vertical normal modes are resonantly excited and we collect data at each BPM electrode for 1024 turns. Three distinct sets of turn-by-turn data are independently fit and combined for this figure. The error bar (nearly invisible) represents the spread in fitted gains for the different data sets.

ment of the  $2Q_x$  signal due to a known change in the field strength of a single sextupole. The measured difference is shown in blue and the calculated difference in red.

Initial studies of the sextupole driven resonances yield measurements in reasonable agreement the theoretical model. Our goal is to use the phase and amplitude of the motion characterized by linear combinations of horizontal and vertical tune (such as  $2Q_x$ ) to measure and correct the field strengths of all sextupoles in the lattice.

## TUNE SCANS OF VERTICAL BEAM SIZE

Our X-ray Beam Size Monitor (xBSM) is capable of measuring bunch-by-bunch, turn-by-turn beam sizes for a

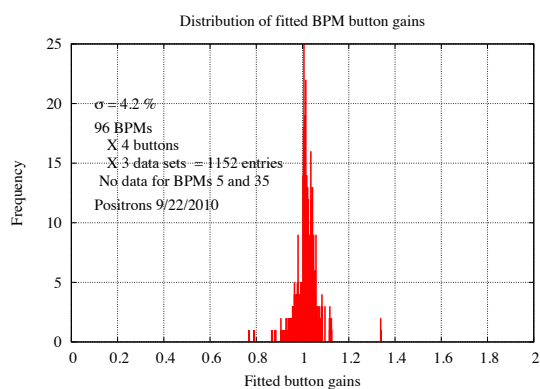


Figure 5: A histogram for the distribution of fitted gains shown in figure 4.

14ns bunch spacing. To reduce the effects of turn by turn jitter, the profile is fitted on each turn to a Gaussian and the standard deviations are averaged over 100 turns. We utilize the xBSM to measure the effects of changing the optics in real-time. We have developed an automated method for scanning the tune plane and sampling the beam size at a specified interval. We use a simple pinhole optic for the xBSM. The pinhole width  $16\mu\text{m}$  determines the resolution limit of the optic. A tune scan was performed on a lattice with sextupole distribution optimized[3] to reduce resonance-driving terms and increase dynamic aperture. We simulate the dependence of beam size on tune by tracking a particle for 1024 turns and determining its maximum vertical amplitude for a specified grid of horizontal and vertical tunes. The simulation includes quadrupole tilt and offset errors of  $\sigma_{tilt} = 200\mu\text{-rad}$  tilts and  $\sigma_{off} = 125\mu\text{m}$ , typical for the present alignment in CESR. Quadrupole strength errors comparable to those typical of the corrected optics are found to have negligible effect on the results.

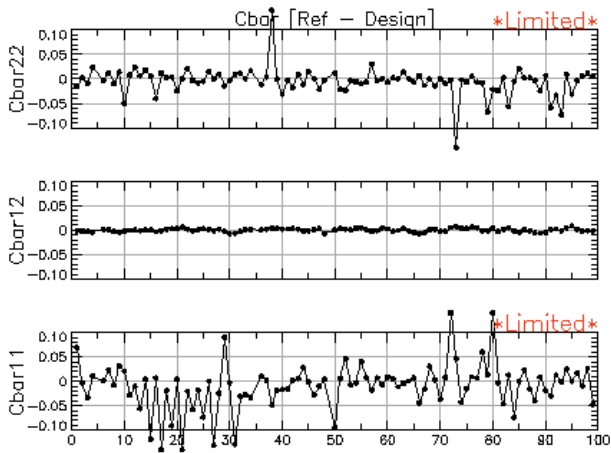


Figure 6: Coupling data after  $\bar{C}_{12}$  correction but before BPM gain corrections.

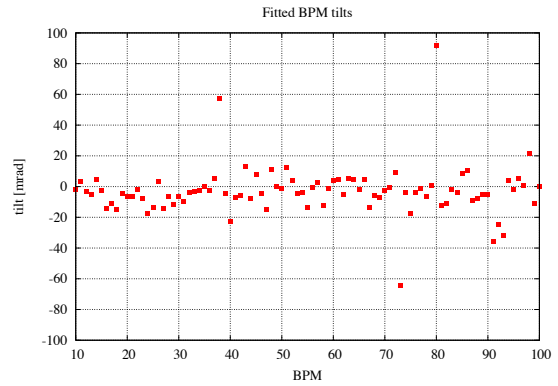


Figure 8: BPM tilts as determined from fitting the gain-corrected coupling data.

## CONCLUSION

In order to identify and compensate sources of vertical emittance it is essential to calibrate and characterize the BPM system. We have reported on the status of a new technique for precisely measuring BPM-quadrupole offsets that is made possible by the CestrTA digital BPM electronics. We show that there is a significant variation in the electrode gains in each BPM, the effect of the gain errors on the coupling measurement, and have successfully compensated for this effect. We are able to extract BPM tilts from the gain-corrected coupling data, and the gain and tilt errors have a non-negligible effect on our measurement of vertical dispersion. Scans of vertical beam size vs betatron tune are used to identify the minimum beam size operating point. Finally, we describe a technique for extracting information about the sextupole optics from turn-by-turn data.

## REFERENCES

- [1] M.Palmer et al., "CESR Beam Position Monitor System Upgrade for CestrTA and CHESS Operations", Proceedings of the 2010 International Particle Accelerator Conference, Kyoto, Japan.
- [2] D.Rubin, M.Billing, R.Meller, M.Palmer, M.Rendina, N.Rider, D.Sagan, J.Shanks, and C.Strohman, Phys. Rev. ST Accel. Beams, 13, 092802 (2010).
- [3] J. Bengtsson, "The Sextupole Scheme for the Swiss Light Source (SLS): An Analytic Approach", SLS Note 9/97

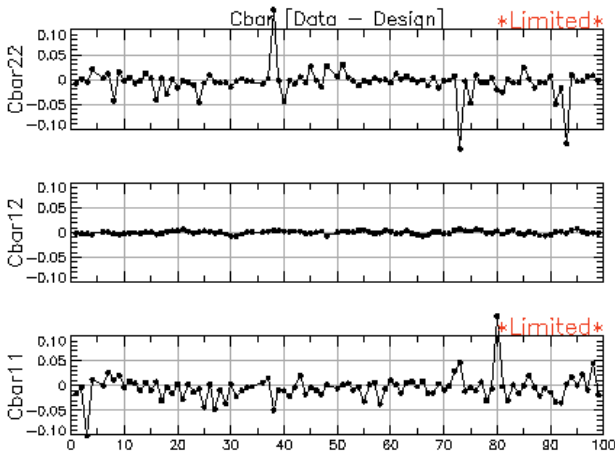


Figure 7: Coupling data after BPM gain corrections.

A tune scan has enabled us to identify the working point corresponding to minimum vertical beam size (and thus emittance). The measured resonance structure is in reasonable agreement with simulation, indicating the sextupoles have had the expected effect.

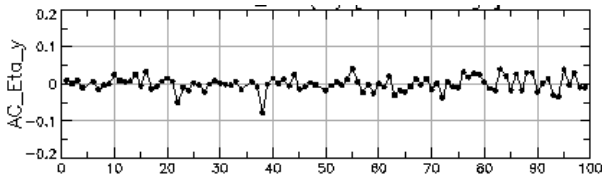


Figure 9: Measured vertical dispersion with no gain or tilt correction. Transverse coupling and vertical dispersion have been jointly minimized through an optimization of skew quadrupoles and vertical steerings. The residual dispersion is 20mm RMS.

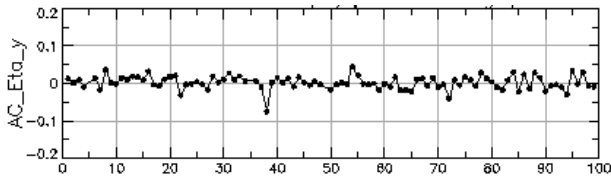


Figure 10: The same measured vertical dispersion, now with BPM button gain corrections. The residual is reduced to 18mm RMS.

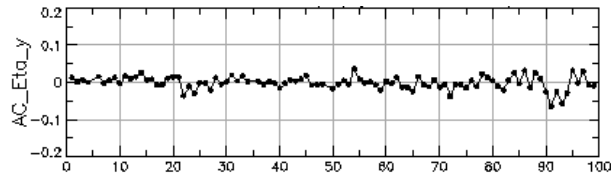


Figure 11: Again, the same measured vertical dispersion with both BPM button gain and BPM tilt corrections. The residual is now reduced to 17mm RMS.

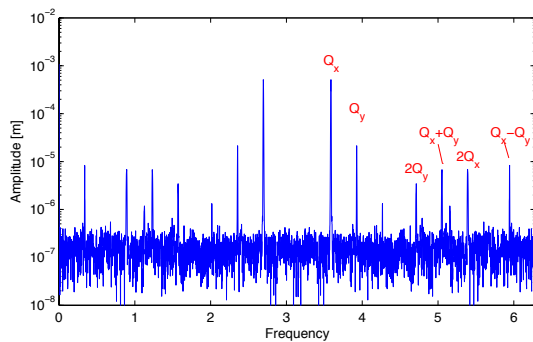


Figure 12: Fourier spectrum of 4096 turns of horizontal turn-by-turn BPM signal.

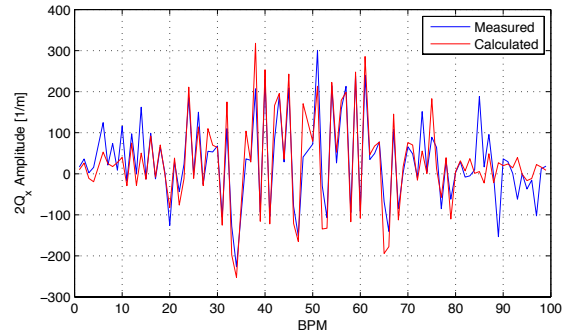


Figure 13: Amplitude of the in-phase response at  $2Q_x$ . The blue line is the measurement and the red the model.

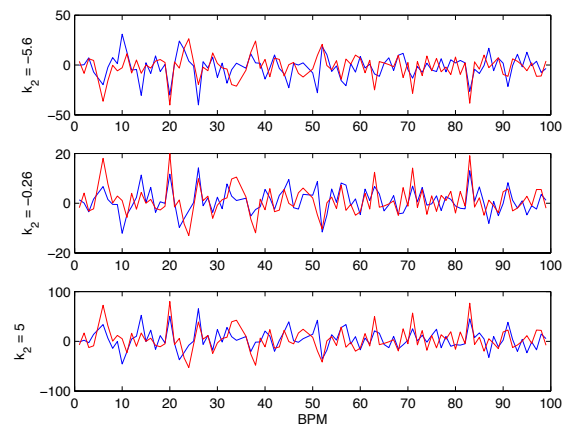


Figure 14: Difference in the in-phase component due to a known change in field strength of a single sextupole. Data is in blue and model in red.

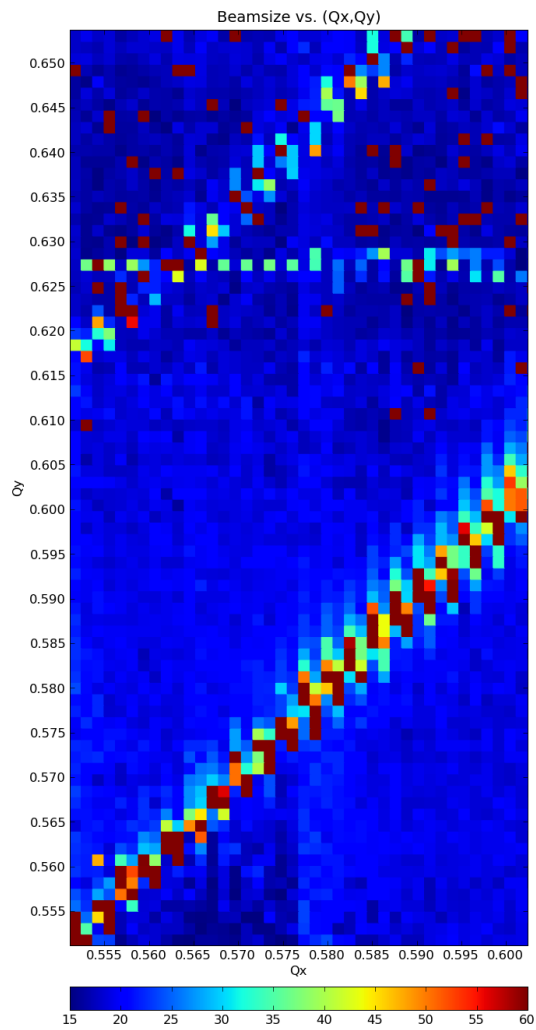


Figure 15: Measured vertical beam size versus horizontal and vertical tune.

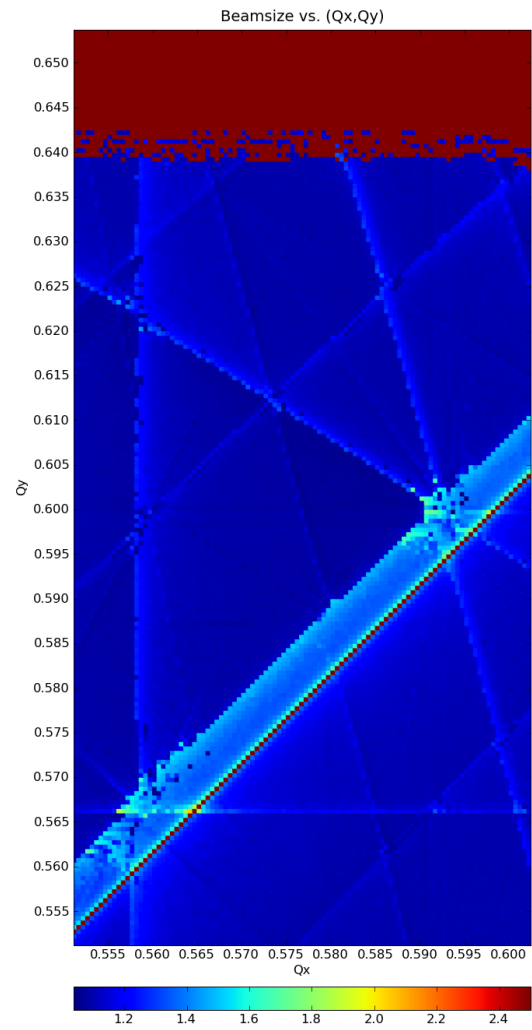


Figure 16: Simulated vertical beam size versus horizontal and vertical tune.